Iraqi National Journal of Chemistry

Journal homepage:
http://iqnjc.com/Default.aspx

New Schiff base metal (II) complexes derived from pyridine-3-carboxaldehyde and an investigation of their biological activities

Rana R. Abed[1]

ranaalbustani@uomosul.edu.iq

University of Mosul / College of Education for Pure Science.

Abstract

New Metal complexes were synthesized and characterized. of Mn $^{++}$, Zn, $^{++}Cd^{++}$, and Hg^{++} for Ligand of Schiff base, 2-methoxy-6-((1E) -((pyridin-3-ylmethylene) hydrazon) methyl) phenol ($C_{15}H_{13}N_3\ O_2$) in ethanol media. The Schiff base was prepared by condensation reaction between OrthoVanillin and hydrazine, then pyridine-3-carboxaldehyde was added to it. Elemental analysis, spectral studies (FT-IR, H^1-NMR, C^{13}-NMR), molar conductance, and melting points were determined for the Ligand and complexes. The Metal complexes having Formula $[M(L)_2\ Cl_2]$, where L = ligand, M = Mn^{++} ,Zn^{++} ,Cd^{++} and Hg^{++} respectively. FT-IR, electronic spectra, and H-NMR data suggested that two nitrogen (N-donor) atoms of the azomethine group, the pyridine molecule, and one Oxygen atom of the hydroxyl group coordinated with metal(II) ions. So, we proposed six coordinated octahedral complexes for Mn, Zn, and Cd, and square-planar complexes for Hg. Also, the results of molar conductance studies showed that Mn and Zn, Cd, and Hg complexes were electrolytic at a (2:1) molar ratio, respectively. Molecular docking is one of the primary tools utilized in drug discovery pipelines. All molecular docking calculations were carried out, and binding modes of docked compounds (L) with protein (1KZN) were determined by MOE software. Schiff base ligand (L) and its metal(II) complexes were screened in vitro against Gram-negative bacteria (Escherichia coli, Pseudomonas aeruginosa) and Gram-positive Bacteria (Staphylococcus aureus) for bactericidal activity using the disc diffusion method. After conducting antibacterial evaluation, it was observed that metal(II) complexes exhibited greater antibacterial activity than the free Schiff base ligand.

Keywords: Schiff base, metal complexes, antibacterial, molecular docking

1 Introduction:

Synthesis and characterization of Schiff base metal complexes with N_2 and O_2 as donor atoms remain an active area of research. Under different reaction conditions, these ligands can bind to a metal atom in different ways. These ligands are formed by the condensation of aldehydes with primary amines [1]. The biological activity of Schiff base metal complexes is one of their most studied areas. The ultimate goal of this research is to find safe and effective drugs used to combat infections and cancers. Many Schiff base metal complexes exhibit various biological and pharmaceutical properties. Transition-metal complexes with Schiff base ligands containing "N2" donor atoms are significant for their biological activities [2]. Molecular docking is one of the primary tools utilized in drug discovery pipelines. All molecular docking calculations were carried out, and binding modes of docked compounds (L) with protein (1KZN) were determined by MOE software [3]. Schiff base ligand (L) and its metal(II) complexes were screened in vitro against Gram-negative bacteria (Escherichia coli, Pseudomonas aeruginosa) and Gram-positive Bacteria (Staphylococcus aureus) for bactericidal activity using the disc diffusion method. After conducting antibacterial evaluation, it was observed that metal(II) complexes exhibited better antibacterial activity [4] than the free Schiff base ligand [5]. This has generated great interest in exploring such systems. In continuation of our ongoing efforts in the synthesis and characterization of metal complexes towards finding potent biological applications. The antibacterial activity of newly synthesized Mn(II), Zn(II), Cd(II), and Hg(II) complexes of the ligand. 2-methoxy-6-((1E)-((pyridin-3-ylmethylene)hydrazono)methyl)phenol ($C_{15}H_{13}N_3O_2$) has been evaluated and reported herein. Antibacterial activity studies revealed that metal complexes, which were predicted to adopt a four-coordinate tetrahedral geometry, exhibited enhanced antibacterial activity compared to the free ligand against Gram-negative bacteria (E. coli and P. aeruginosa) and Gram-positive bacteria [6]. (B. subtilis and S. typhi).

2. Matereals and Method

The synthesis of the Schiff base ligand (L) was carried out according to the literature method with some modifications [7]. OrthoVanillin (9.88 g; 0.065 mol) was added to a stirred ethanolic solution (40 ml) of Hydrazine (2.08 g; 0.065 mol) at a (1: 1) molar ratio. 2-3 drops of acetic acid were added to the reaction mixture to adjust its pH to ≃6. Then refluxed for 3 hours. Immediately, a thick yellow precipitate was obtained. The precipitate was separated and purified by recrystallization. Yellow crystals were formed. Yield: 85.0%; color: yellow; m.p. = 144–145°C; $C_8H_{10}N_2O_2$ (FW = 166). Then, Pyridin-3-carboxaldehyde (3.22 g; 0.030 mol) was added to a stirred ethanolic solution at a (1: 1) molar ratio to dryness in a round-bottomed flask at room temperature. 2-3 drops (0.2 mL) of acetic acid were added to the mixture. Upon addition, a thick yellow-orange precipitate formed immediately. Then, it was refluxed for 3 hours [8]. The precipitate obtained was filtered and purified by recrystallization. The product obtained was washed with ethanol and diethyl ether to remove unreacted amine and aldehyde. Then dried in air. Yield: 84.0%, m.p = 226-227°C, $C_{14}H_{13}N_3O_2$ (FW = 255) (Scheme 1).

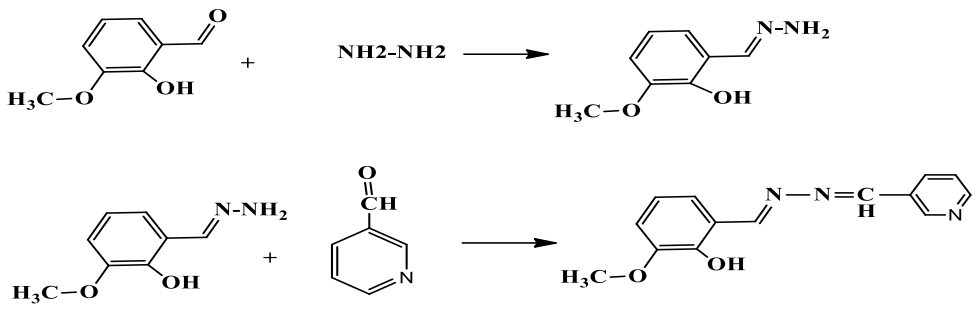

(Scheme 1)

The complexes (Scheme 2) were prepared by mixing the salts with the ligand in a (1:2) ratio using literature procedures [9]. Solution of hydrated metal(II) (0.0018 mol) in ethanol-water solvent (10 mL) at 60 °C was added dropwise to a solution of ligand (L) (0.0036 mol) in ethanol solvent (10 mL) at 50°C with magnetic stirring in a round-bottom flask. The solution was refluxed at 80 C° for 5 hours with continued magnetic stirring. The separated solid was filtered and washed with distilled water and diethyl ether. (Scheme 2). Table 1 explains the molecular weights, molecular formulas, and some physical characteristics [10].

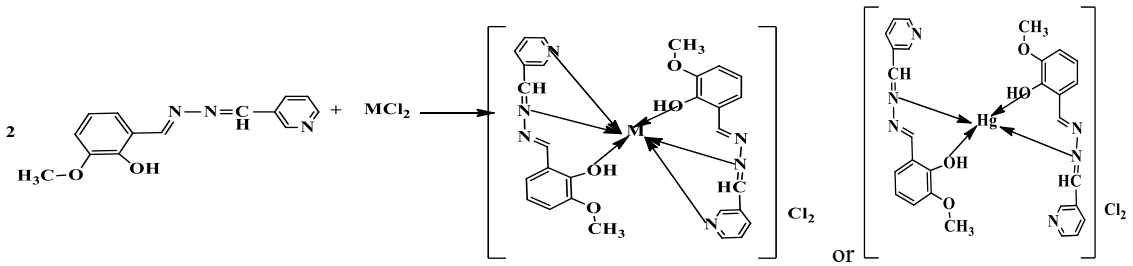

(Scheme 2)

Table 1: weights, molecular formulas, and some physical characteristics

no	Salt	w.t of salt gm	w.t of Lgm	Structure	Color	M.wt	m.p	conductivity
1	$MnCl_2.2H_2O$	0.5	0.64	$[Mn(C_{28}H_{26}N_6O_4)Cl_2]$	yellow	635.9	229-230	-
2	$ZnCl_2$	0.5	0.93	$[Zn(C_{28}H_{26}N_6O_4)Cl_2]$	light yellow	646.3	323-324	77
3	$CdCl_2$	0.5	0.69	$[Cd(C_{28}H_{26}N_6O_4)Cl_2]$	light yellow	693.41	338-339	75
4	$HgCl_2$	0.5	0.46	$[Hg(C_{28}H_{26}N_6O_4)Cl_2]$	yellow	781.59	337-338	78

3. Results

The Schiff base ligand was previously synthesized via reflux [11]. The synthesized complexes were new and have been prepared for the 1st time here. The ligand was soluble in ethanol and dimethylformamide. The metal (II) complexes were colored solids, stable in air. insoluble in methanol, dichloromethane, and acetone. The melting points of the complexes were observed to be higher than those of the ligand, indicating that the metal complexes are more stable than the ligand. The molar conductance values of the synthesized complexes were measured in 10^{-3} M DMSO at room temperature. The measured conductance values of synthesized compounds were less than73-78 Ohm −1 cm^2 mol^{-1}, which clearly indicates their electrolytic [1: 2] nature [12]. This could be explained by the presence of Cl_2 anions that were outside the coordination sphere of the complexes. The microanalysis data revealed that all the complexes were mononuclear, with two moles of the ligand attached to the central metal atom through donation of a lone pair of electrons to two nitrogen donor atoms and one Oxygen atom coordinated to the metal (II) ions. Hence, the metal: ligand ratio for the complexes was found to be 1: 2 and the molecule structure for all the synthesized complexes could be written as $[M(L)_2]Cl_2$ (M = Mn^{++}

Zn^{++}, Cd^{++}, and Hg^{++}, six-coordinated octahedral geometry complexes for Mn, Zn, Cd complexes, and square planar geometry for Hg complex [13]. The theoretical (calc) values matched the experimental values very well.

Table 2: Elemental analysis for ligand and complexes

No.	Structure	Yield%	C%cal(exp)	H% cal(exp)	N% cal(exp)	M% cal(exp)
L	$C_{14}H_{13}N_3O_2$	87	65.88(66.03)	5.09 (5.59)	16.47(16.50)	-
1	$[Mn(C_{28}H_{26}N_6O_4)Cl_2]$	69	52.83(52.53)	4.08(5.00)	13.20(12.88)	8.63(8.55)
2	$[Zn(C_{28}H_{26}N_6O_4)Cl_2]$	76	51.98(52.01)	4.02(4.69)	12.99(13.05)	10.10(11.05)
3	$[Cd(C_{28}H_{26}N_6O_4)Cl_2]$	83	48.45(49.00)	3.74(4.01)	12.11(12.71)	16.21(15.87)
4	$[Hg(C_{28}H_{26}N_6O_4)Cl_2]$	76	42.98(42.23)	3.32 (4.23)	10.74(11.12)	25.66(24.79)

4 FT-IR

In FT-IR spectroscopy The possible way of attachment of the ligand to metal ions in synthesized complexes were assigned on the basis of comparison between FT-IR spectrum of the free ligand and those of the metal (II) complexes. The band at 1593.31 cm^{-1} for free ligand due to (υ C=N) . Shift of the C=N stretching frequencies to lower frequency for metal (II) complexes confirmed the coordination of nitrogen atom of Schiff base to metal [14], strong band is observed at 3403.26 cm^{-1} belong to 2 of (υ O-H) group on of this band shifted to lower frequency that indicated coordination of Oxygen atom for phenolic group to the metal ion, strong band is observed at

1336.42 cm^{-1} belong to 2 of (υ C-$P_{yridine}$) group on of this band shifted to lower frequency that indicated coordination between Nitrogen atom of pyridine and metal ion except mercury complex the band stay on same position that indicated there is no coordination between Nitrogen atom and mercury ion, Further, shifting of bands and the appearance of some new weak bands at the region 427.22-444.73, cm−1 belong to (υ M-N) in complexes [15]. which further confirms the complexation. Infrared spectroscopy of the complexes also exhibited bands in the 541.61- 619.19 cm^{-1} region, which accounts for the coordinated Oxygen atom and metal ion (υ M-O) complexes.

Table 3: The most important bands in Infrared spectroscopy

No.	C=N	OH phenolic	C-N Pyridine	C-H Ar	M-N	O-M
L	1593.31	3403.26	1336.42	3091.96	-	-
1	1579.87	3351.65	1307.14	3064.63	541.61	427.22
2	1578.01	3331.92	1329.61	3145.86	619.19	467.87
3	1579.83	3353.50	1330.92	3081.43	557.80	440.87
4	1578.06	3356.28	1332.72	3087.16	558.53	444.73

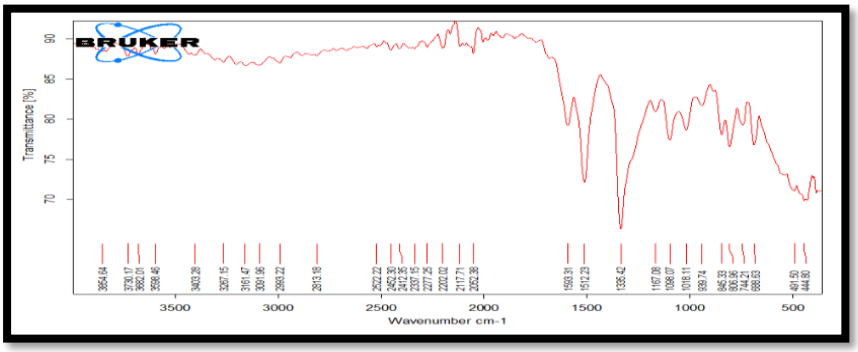

Fig 1 Infrared spectroscopy for Ligand

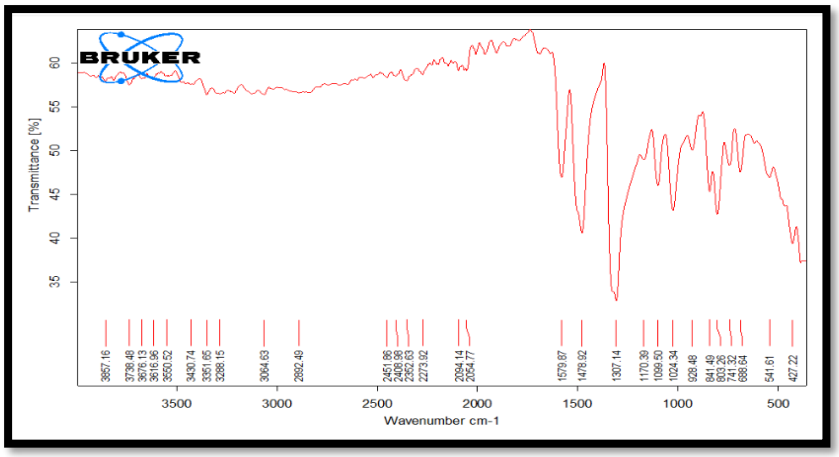

Fig. 2: FT-IR of complex no1 1

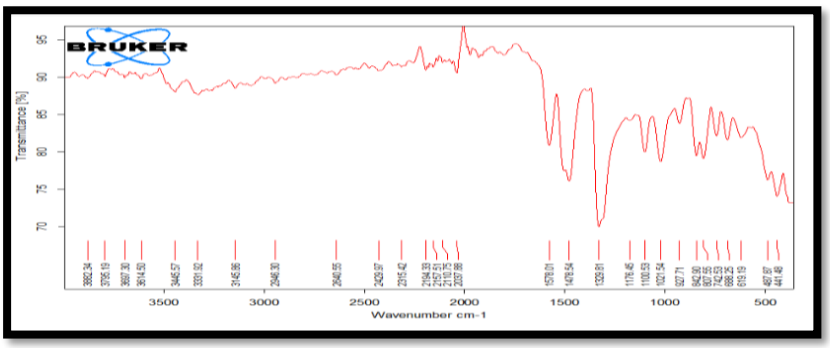

Fig. 3: FT-IR of complex no.2

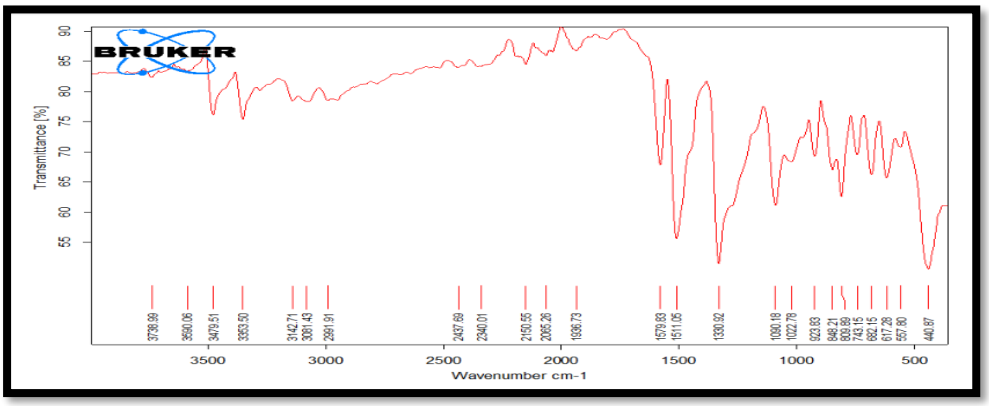

Fig. 4: FT-IR of complex no.3

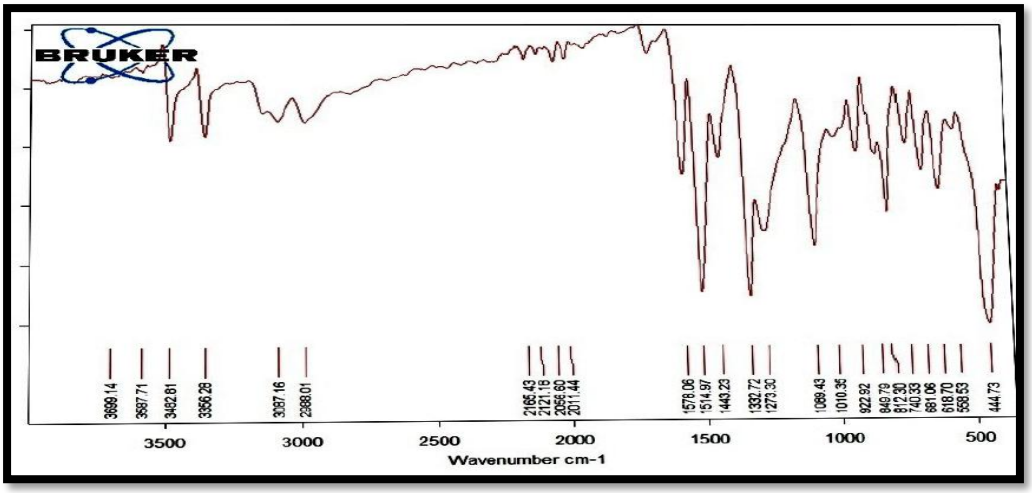

Fig. 4: FT-IR of complex no.4

4. ^{1}H-NMR Spectral Analysis

1H NMR spectra of the ligand were measured in deuterated DMSO-d6. ^{1}H-NMR spectrum of L showed a singlet at δ 7.87 ppm, assigned to the azomethine proton (–N=CH–), confirming the formation of the Schiff base after the condensation reaction. singlet peak at δ =6.84- 7.67ppm corresponds to protons of aromatic ring. The singlet peak at δ = 4.83 ppm corresponds to the methoxy group, and the singlet peak at δ = 5.40 ppm corresponds to the hydroxyl group [16].

Fig. 5: HNMR of Schiff base ligand

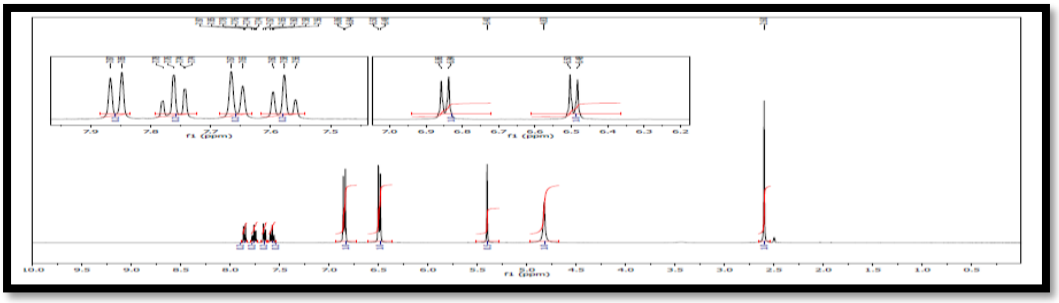

^{13}C-NMR Spectral Analysis

13C NMR spectra of the ligand were measured in deuterated DMSO-d^{6} solvent. From the ^{13}C NMR spectrum of the ligand, a singlet peak was observed at δ = 170.75 ppm, corresponding to the azomethine Carbon (–N = CH–) [17]. This proves that Ligand exhibits multiple peaks at δ = 113. -134. ppm belong to the carbons of the aromatic ring. multi peaks at δ =147.34-146.38. 8 ppm belongs to the carbon of the hydroxyl group. Multi peaks at δ =69.94 ppm belong to the carbon of the methoxy group.

.

Fig. 5: C^{13}NMR of Schiff base ligand

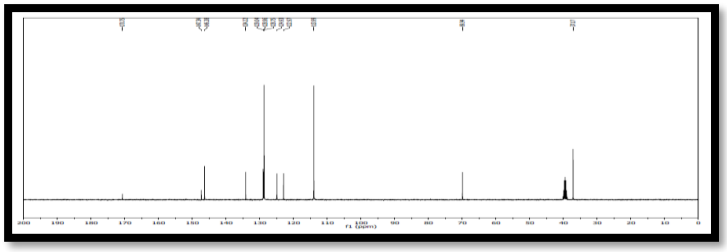

MASS SPECTRA: The mass spectrometry spectrum of the prepared compound was recorded to determine the molecular mass and study the fragmentation pattern that supports the proposed structure of the ligand.

Fig 7 XRD of ligand

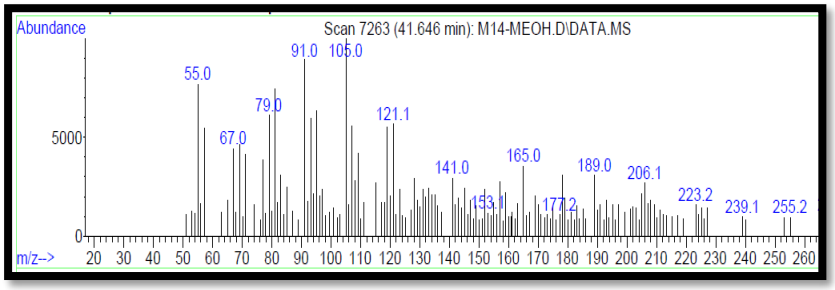

XRD :

The X-ray Diffraction (XRD) pattern of the prepared compound was recorded to study its crystalline nature and determine the peak positions at 2θ. Figure (7) shows the diffraction pattern, while Table (4) shows the calculated values of 2Ɵ and d-spacing and the intensities of the peaks.

Fig 7 XRD of ligand

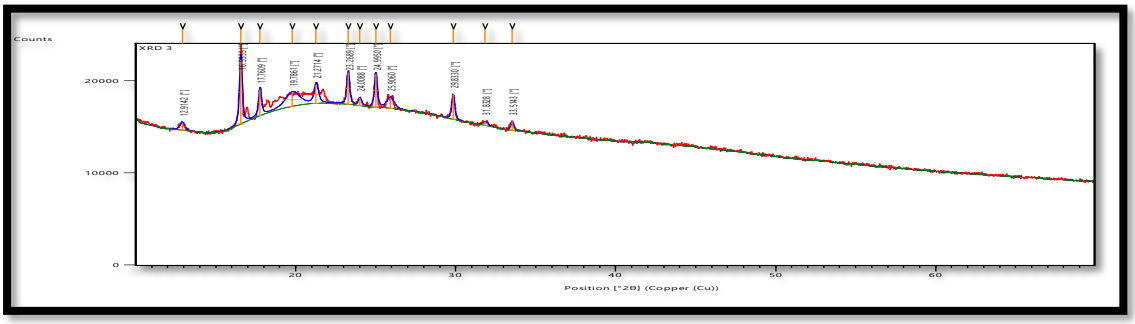

Table 4

Pos. [°2θ]	Height [cts]	FWHM Left [°2θ]	d-spacing [Å]	Rel. Int. [%]	Tip Width
12.9142	784.53	0.3582	6.85528	11.28	0.4298
16.5555	6952.74	0.2047	5.35477	100.00	0.2456
17.7609	2800.53	0.2047	4.99398	40.28	0.2456
19.7861	1428.88	1.0234	4.48715	20.55	1.2280
21.2714	1994.58	0.3070	4.17708	28.69	0.3684
23.2689	3429.76	0.2047	3.82282	49.33	0.2456
24.0088	799.15	0.2047	3.70666	11.49	0.2456
24.9950	3585.67	0.2047	3.56261	51.57	0.2456
25.9060	1114.66	0.5117	3.43936	16.03	0.6140
29.8330	2683.67	0.2047	2.99497	38.60	0.2456
31.8328	401.36	0.3070	2.81123	5.77	0.3684
33.5143	956.52	0.2047	2.67393	13.76	0.2456

3 Study of Molecular Docking

The structure of the proteins (1KZN) (fig 3) was retrieved from the Protein Data Bank. Since the water molecule in the active sites of target proteins functions critically, it was included in the active sites to enable hydrogen bonding between L and the target. Afterward, the protein structure was prepared, correcting missing bonds (perhaps broken in XRD) and adding hydrogen atoms. (Figure 3b). Interestingly, the Protein Data Bank is a globally accepted source of crystal structure information for biological macromolecules [18].

Ligand–Protein molecular docking

All Docking was performed using molecular operation environment software (MOE) ((MOE), Molecular Operating Environment (2022)). Protein crystal structure (hereby referred to as 1KZN) (Figure 3) was downloaded from the RCSB Protein Data Bank with a resolution of 2.30 Å. Protein-ligand docking studies with resolutions of 1.5-3.5 Å are reported to yield high-quality results. It has been experimentally observed that the ideal RMSD should be around 2 Å and the energy score ≤ −7 kcal/mol. The best score is determined by these two parameters, which are commonly used to validate the docking results. Molecular docking serves as an important tool in the drug discovery process [19]. Molecular docking calculations were performed using MOE software to predict binding modes of all prepared compounds (L2) with protein (1KZN) (Figure 3). Predicted binding affinities and properties of the studied compound (L2) against (1KZN) are mentioned in the next tables. The table shows the best binding poses obtained by compound (L2) against target proteins. The figures and tables below show 2D and 3D representations of interactions between the inspected

compound and key amino acid residues in the (1KZN) protein. As shown in Table 2 and Table 3, compound (L2) has good binding affinity for protein (1KZN). Interaction in 2D and 3D modes of the compound (L2) with the (1KZN) protein. From this interaction, it can be concluded that several types of interactions are involved, including hydrogen bonding and hydrophobic interactions [20]. All interactions were investigated for bond lengths and hydrogen bonds at the active site in the figures below. Figures showed that the studied compound (L2) formed interactions with various amino acids across three types: H-donor, H-acceptor, and H-pi. Also, there were two types of interactions occurring between water molecules, different amino acids, and the target protein, including H-acceptor and pi-H. The distance and energy binding for each interaction are listed in the tables below [21].

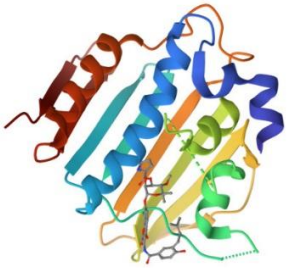

Figure 3: Crystal structure of the selected protein

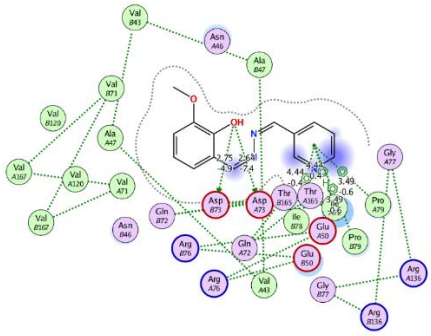

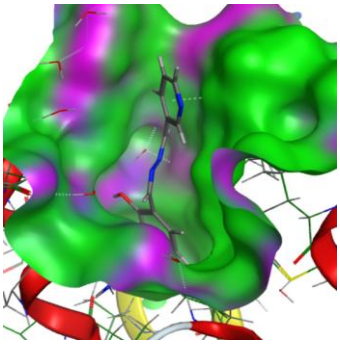

Fig 4 Ligand-pose1

Table 5: The binding affinity and RMSD results of the **1KZN** protein from the docking process

Compounds	mseq	Binding Affinity Kcal/mol	Rmsd (Å)	E_conf	E_place	E_score1	E_refine	E_score2
L2-pose1	1	-7.17902	1.454962	45.03647	-12.5414	-10.2273	-39.0112	-7.17902
L2-pose2	1	-6.9397	1.291576	45.95923	-14.5715	-11.2106	-34.6182	-6.9397
L2- pose 3	1	-6.91615	1.198185	51.15868	-11.9099	-10.8545	-35.0017	-6.91615
L2- pose 4	1	-6.79756	0.989969	49.28842	-15.6764	-10.0982	-33.0188	-6.79756
L2- pose 5	1	-6.66536	1.592055	46.06509	-12.9759	-12.2246	-34.4116	-6.66536
Standard:tetracycline	std	-6.98236	1.9261	19.61369	-76.748	-9.8539	-31.4543	-6.98236

3. Antibacterial activity

The antibacterial activity was evaluated using a standard procedure against two Gram-positive and two Gram-negative bacterial strains [22]. The results obtained are listed in Table 3. The

antibacterial activities of the Schiff base ligand and its metal(II) complexes were studied and compared with the standard antibacterial drugs Amoxicillin-Clavulanic Acid (AMC) and Gentamicin (GEN). It was concluded that the ligand and its complexes exhibited inhibitory activity against bacterial growth. It has been reported that the ligand coordination exhibited antibacterial growth-inhibitory properties [23]. From the inhibition zones of the Schiff base ligand and its complexes at different concentrations, it can be concluded that the complexes exhibit better bactericidal activity than the ligand [24] and the standard antibiotic amoxicillin-clavulanic acid (AMC) against all tested bacteria. Metal complexes show increased activity with increasing concentration. Various theories were proposed to explain the biological activity of transition-metal coordination compounds. The Increased antibacterial activity of metal(II) complexes may be due to metal-ion binding to the bacterial cell and disruption of its normal state [25]. Reportedly, a structural moiety containing additional (C=N) and (C-N py) nitrogen-donor atom systems can inhibit enzyme activity through deactivation upon coordination to metal centers. According to Tweedy's chelation theory, the overlap of ligand orbitals causes a significant reduction in the metal ion's polarity through partial sharing of the metal ion's positive charge with donor groups [26]. Hence, it can be concluded that these complexes may be useful and reasonably used in the design of potent antibacterial drugs to treat diseases caused by P. aeruginosa, E. coli, and S. typhi [27].

Table 6: The inhibition zones for ligand and complexes

Bacteria	***E. coli***			***P. aeruginosa***			***S. typhi***		
Con. μg/mL.	**500**	**250**	**125**	**500**	**250**	**125**	**500**	**250**	**125**
L	**25**	**12**	**9**	**10**	**7**	**-**	**21**	**8**	**6**
1	**26**	**14**	**10**	**8**	**-**	**-**	**9**	**6**	**-**
2	**22**	**10**	**9**	**21**	**8**	**6**	**22**	**12**	**10**
3	**23**	**20**	**16**	**21**	**18**	**10**	**20**	**13**	**8**
AMC	**13**			**12**			**13**		
GEN	**12**			**12**			**12**		

(AMC)= Amoxyclav, and (GEN)= Gentamicin

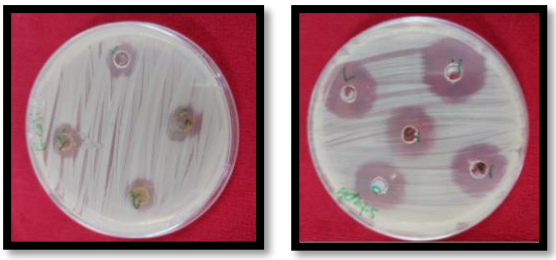

Fig. 8: inhibition zones of Ligand and complexes

4 Conclusion

Schiff base ligand, 2-methoxy-6-((1 E)-((pyridin-3-ylmethylene) hydrazono)methyl) phenol ($C_{15}H_{13}N_3O_2$) and its complexes {$[M(L)_2]Cl_2$; (M = Mn (II), Zn (II), Cd (II) and Hg(II) } were synthesized and characterized. The Schiff base ligand, after deprotonation, chelated with a metal (II) ion through the nitrogen atom of the azomethine group, the nitrogen of the pyridine, and the oxygen atom of the phenolic group, thereby forming a stable five- and six-membered chelate ring. The metal(II) complexes were reported to have octahedral geometry, and the Hg(II) complex was reported to have square-planar geometry [28]. The metal complexes have shown greater antibacterial activity than the ligand under the same conditions. It could also be concluded from the study of the ability of all compounds to inhibit growth that increasing concentration results in greater inhibition.

References

[1] FALLAH-MEHRJARDI, Mehdi, et al. A review of bidentate NN and NO Schiff base ligands and metal complexes. *Inorganica Chimica Acta*, 2025, 587: 122822.

https://doi.org/10.1016/j.ica.2025.122822

[2] MUSHTAQ, Irfan, et al. Pharmaceutical significance of Schiff bases: an overview. *Future Journal of Pharmaceutical Sciences*, 2024, 10.1: 16.

https://doi.org/10.1186/s43094-024-00594-5

[3] SANDHU, Qurat-Ul-Ain, et al. Schiff base metal complexes as anti-inflammatory agents. *Journal of Coordination Chemistry*, 2023, 76.9-10: 1094-1118.

https://doi.org/10.1080/00958972.2023.2226794

[4] GANESAN, Muthuraj; AROCKIASAMY, Sebastian. A review of titanium (IV) complexes of Schiff base ligands and their derivatives containing the donor atoms ONO, ONON, ONNO, and heterocyclic exhibiting biological activity covered over two decades along with the significance of molecular docking. *Discover Chemistry*, 2025, 2.1: 7.

https://doi.org/10.1007/s44371-024- 00064-0

[5] AKBARI, Zahra, et al. Biological evaluation, DFT, MEP, HOMO-LUMO analysis and ensemble docking studies of Zn (II) complexes of bidentate and tetradentate Schiff base ligands as antileukemia agents. *Journal of Molecular Structure*, 2024, 1301: 137400.

https://doi.org/10.1016/j.molstruc.2023.137400

[6] SEVERIN, Tobias, et al. Synthesis, Structures and Photophysical Properties of Tetra-and Hexanuclear Zinc Complexes Supported by Tridentate Schiff Base Ligands. *Chemistry*, 2023, 5.2: 1028-1045.

https://doi.org/10.3390/chemistry5020070

[7] TSANTIS, Sokratis T., et al. Two different coordination modes of the Schiff base derived from ortho-vanillin and 2-(2-aminomethyl) pyridine in a mononuclear uranyl complex. *Heliyon*, 2022, 8.6.

https://doi.org/10.1016/j.heliyon.2022.e09705

[8] VASSILYEVA, Olga Yu, et al. Heterometallic CuCd and Cu 2 Zn complexes with o-vanillin and its Schiff-base derivative: slow magnetic relaxation and catalytic activity associated with Cu (ii) centres. *Dalton Transactions*, 2025, 54.15: 6117-6132.

DOI: 10.1039/D4DT03571B

[9] SUMAYYA, I. B., et al. SYNTHESIS, CHARACTERIZATION, AND ANTIOXIDANT ACTIVITY ON METAL (II) COMPLEXES OF A SCHIFF BASE DERIVED FROM THIOSEMICARBAZIDES AND O-VANILLIN. *Science World Journal*, 2025, 20.4: 1438-1442.

https://dx.doi.org/10.4314/swj.v20i4.16

[10] BARIYA, Dipakkumar, et al. Aminopyridine-Vanillin Schiff Base as a Turn On Fluorescent Sensor for Highly Selective Zn (II) Metal Detection. *Luminescence*, 2025, 40.9: e70305.

https://doi.org/10.1002/bio.70305Digital Object Identifier (DOI)

[11] GANJEGAONKAR, S. B.; DESHMUKH, J. H.; PAWAR, P. A. Synthesis, IR, and NMR Study of Some Cu (II), Ni (II), Co (II) Complexes of O-Vanillin and 2-Amino Pyridine. *Oriental Journal of Chemistry*, 2022, 38.4: 1018.

DOI:10.13005/ojc/380425

[12] ABDULLAH, Qasim Rabeea; MUSTAFA, Ziyad Muhammad. Synthesis and characterization of new Schiff bases complexes with ions elements (Co (II), Ni (II), Cu (II) Mn (II), Zn (II),) and evaluation of the bacterial activity. *International Journal of Health Sciences*, 2022, 6.S3: 10849-10871.

. https://doi.org/10.53730/ijhs.v6nS3.

[13] NASIF, Vesim; SAYIN, Koray. Synthesis of new pyridine based ONNO type schiff bases and Cd (II) complexes, investigation of structural, electronic and anti-cancer properties as computationally and experimentally. *Journal of Molecular Structure*, 2025, 1322: 140359.

https://doi.org/10.1016/j.molstruc.2024.140359

[14] KEBUKAWA, Yoko. Infrared Spectroscopy. In: *Encyclopedia of Astrobiology*. Berlin, Heidelberg: Springer Berlin Heidelberg, 2023. p. 1441-1442.

[15] ABDEL-RHMAN, Mohamed H., et al. New Schiff base ligand and some of its coordination compounds: synthesis, spectral, molecular modeling and biological studies. *Journal of Molecular Structure*, 2023, 1279: 135023.

https://doi.org/10.1016/j.molstruc.2023.135023

[16] GEBREZGIABHER, Mamo, et al. Understanding More on the Coordination Nature of a Series of Lanthanum Complexes from Schiff Bases of Salicylaldehyde Origin by 1H NMR Investigations. *Chemistry Africa*, 2025, 8.2: 579-590.

https://doi.org/10.1007/s42250-024-01168-x

[17] BURAN, Kerem. Metal complexes of sulfamethazine/benzoin-based Schiff base ligand: synthesis, characterization, DFT calculations, and antimicrobial activities. *Turkish Journal of Biology*, 2025, 49.1: 118-126.

. https://doi.org/10.55730/1300-0152.2729

[18] MORIWAKI, Hirotomo, et al. FMOe: Preprocessing and visualizing package of the fragment molecular orbital method for Molecular Operating Environment and its applications in covalent ligand and metalloprotein

analyses. *Journal of Chemical Information and Modeling*, 2024, 64.18: 6927-6937. https://doi.org/10.1021/acs.jcim.4c01169

[19] KONYAR, Dilan; OKUR, Hayati; ARSLAN, Zehra. Molecular docking studies of cox inhibitors on wild-type ras. *Journal of Faculty of Pharmacy of Ankara University*, 2022, 46.1: 23-34.

https://doi.org/10.33483/jfpau.1008048

[20] VENKATESH, Ganesan, et al. Synthesis and spectroscopic characterization of Schiff base metal complexes, biological activity, and molecular docking studies. *ACS omega*, 2024, 9.7: 8123-8138.

https://doi.org/10.1021/acsomega.3c08526

[21] ISMAIL, Hussein Ahmad; ABED, Rana R. Synthesis, characterization, and biological activity assessment of new metal complexes of Schiff bases produced from benzoin. *Al-Kitab Journal for Pure Sciences*, 2023, 7.01: 27-41.

DOI:https://doi.org/10.32441/kjps.07.01.p3

[22] TAWFIQ, K. M., et al. Synthesis, characterization, molecular docking, cytotoxicity, and antimicrobial activity of Schiff base ligand and its metal complexes. *Applied Organometallic Chemistry*, 2025, 39.1: e7781.

https://doi.org/10.1002/aoc.7781Digital Object Identifier (DOI)

[23] ISLAM, Md Ashraful, et al. Experimental and computational insights into antibacterial and antioxidant properties of metal complexes with isoniazid-based Schiff base ligands. *Journal of Molecular Structure*, 2025, 1324: 140916.

https://doi.org/10.1016/j.molstruc.2024.140916

[24] CAVIGLIA, Miriam, et al. New Cu (II), Cu (I) and Ag (I) complexes of phenoxy-ketimine schiff base ligands: synthesis, structures and antibacterial activity. *Molecules*, 2025, 30.9: 1893.

https://doi.org/10.3390/molecules30091893

[25] KARGAR, Hadi; FALLAH-MEHRJARDI, Mehdi; MUNAWAR, Khurram Shahzad. Recent Advances in the Antimicrobial Activity of Zn (II) Schiff Base Complexes. *Inorganic Chemistry Research*, 2025, 9.1: 91-107.

10.22036/j10.22036.2025.553444.1197

[26] SINDHU, Indu, et al. Synthesis, spectral characterization, antimicrobial activity, DFT calculations, molecular docking and ADME studies of novel schiff base Co (II), Ni (II), Cu (II) and Zn (II) complexes derived from 4-nitro-ortho-phenylenediamine. *Chemistry & Biodiversity*, 2025, 22.3: e202402619.

https://doi.org/10.1002/cbdv.202402619

[27] SINDHU, Indu, et al. Synthesis, Characterization, and DFT Investigation of Innovative Schiff Base Transition Metal Complexes: Molecular Docking and Antimicrobial Activity. *Applied Organometallic Chemistry*, 2025, 39.8: e70303.

https://doi.org/10.1002/aoc.70303Digital Object Identifier (DOI)

[28] EL-BORAEY, Hanaa A., et al. Designing of some VO (II), Co (II) and Hg (II) Schiff base complexes: Synthesis, structure elucidation, anticancer and biopesticidal activities, DFT and docking approaches. *Results in Chemistry*, 2024, 11: 101767.

https://doi.org/10.1016/j.rechem.2024.101767